

The impact of triangularity on plasma confinement: TCV experiments vs non-linear gyrokinetic modelling



A. Marinoni, S. Brunner, Y. Camenen, S. Coda, J. P. Graves, M. Jucker, X. Lapillonne, A. Pochelon, O. Sauter, L. Villard and the TCV Team

34th European Physical Society
Conference on Plasma Physics
Warsaw, Poland 2007
Poster P1.067

Ecole Polytechnique Fédérale de Lausanne (EPFL), Centre de Recherches en Physique des Plasmas
Association Euratom-Confédération Suisse, CH-1015 Lausanne, Switzerland

alessandro.marinoni@epfl.ch

Experimental evidence [1]

The Tokamak à Configuration Variable can sustain the following shapes

- Highest triangularities achieved 1 and -0.7
- Maximum elongation achieved 2.8
- Installed ECRH power 4.3 MW

⇒ The influence of plasma shape on electron transport can thus be investigated

Experimental results

- Core transport studied in EC L-mode (to avoid ELM activity)
- $\beta = 2\mu_0 \langle P \rangle / B_0^2 \simeq 10^{-3}$
- χ_e computed from steady-state power balance
- χ_e increases with δ and ν_{eff}
- τ_E doubles when passing from $\delta = 0.4$ to $\delta = -0.4$

The GS2 code[2]

- Flux-tube, Vlasov-Maxwell system of equations solved as an initial value problem ballooning representation for linear terms, explicit flux tube domain treatment for non-linear terms
- The code can handle different ion species
- Collisions (a diffusion pitch-angle operator has been used in this work)
- Fully electromagnetic (electrostatic limit used here)

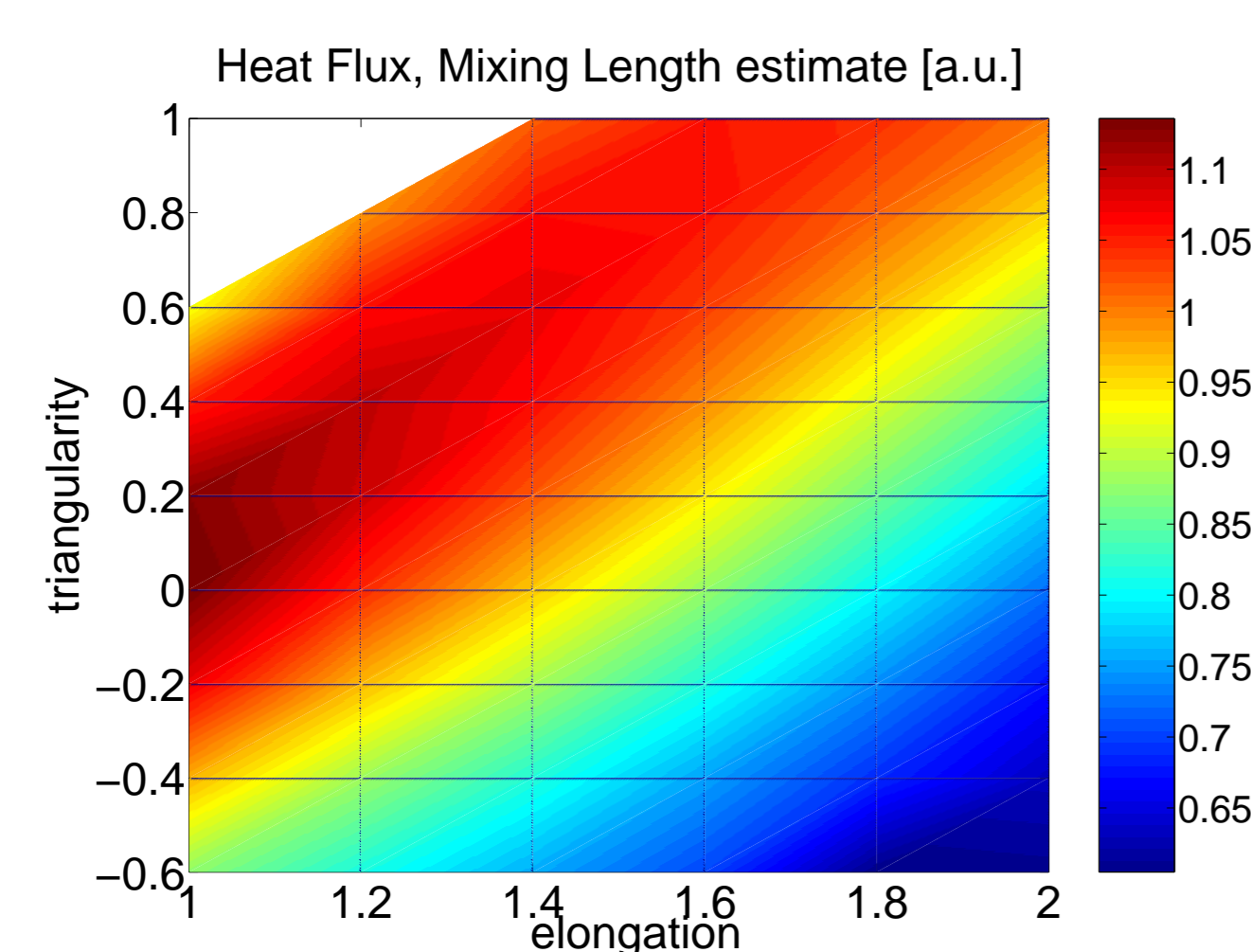
$$\frac{\partial \tilde{f}}{\partial t} + \frac{c}{B} [J_0(k_{\perp} \rho_i) \tilde{\phi} \tilde{f} - \tilde{f} J_0(k_{\perp} \rho_i) \tilde{\phi}] + v_{\parallel} \mathbf{b} \cdot \nabla \tilde{f} + i\omega_d \tilde{f} = i\omega^* J_0(k_{\perp} \rho_i) \tilde{\phi} - e \frac{\partial F_0}{\partial E} \frac{\partial J_0(k_{\perp} \rho_i) \tilde{\phi}}{\partial t} \quad (1)$$

$$\nabla_{\perp}^2 \tilde{\phi} = 4\pi \Sigma_{sp} e \int d\mathbf{v} \left[e \tilde{\phi} \frac{\partial F_0}{\partial E} + J_0(k_{\perp} \rho_i) \tilde{f} \right] \quad (2)$$

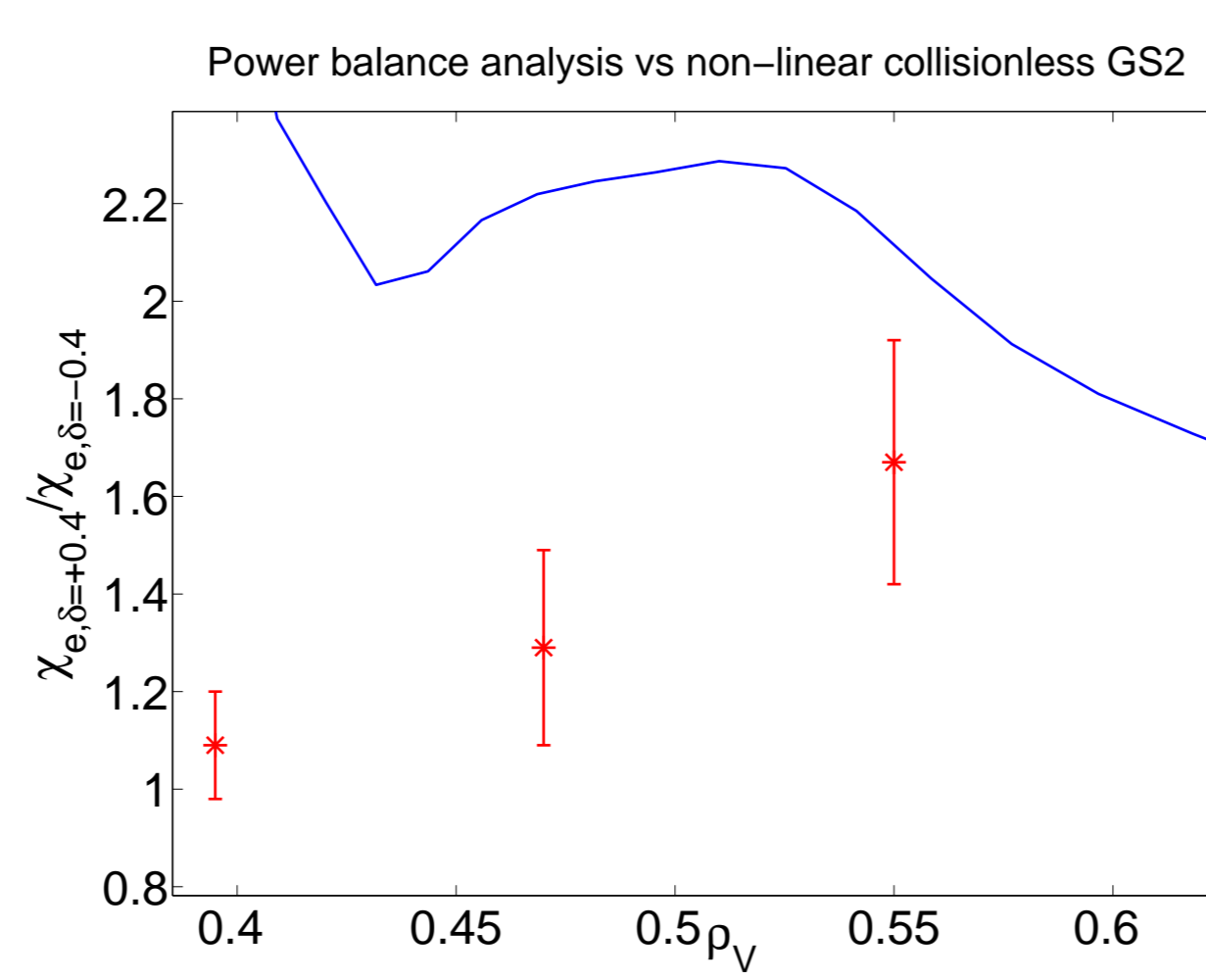
- ω^* is the diamagnetic drift
- $\omega_d = 1/(Bm\Omega) \mathbf{k}_{\perp} \cdot \mathbf{B} \wedge (mv_{\parallel}^2 \mathbf{b} \cdot \nabla \mathbf{b} + mv_{\perp}^2 / (2B) \nabla B$
- \tilde{f} is the non adiabatic part of the distribution function, E is the particle kinetic energy and $\tilde{\phi}$ is the perturbed electrostatic potential

Gyro-kinetic modelling

- The impact of triangularity is observed in linear simulations, both linearly and non-linearly



Estimated diffusivity through a mixing length scaling [3] of a number of linear collisionless GS2 simulations as a function of triangularity and elongation.



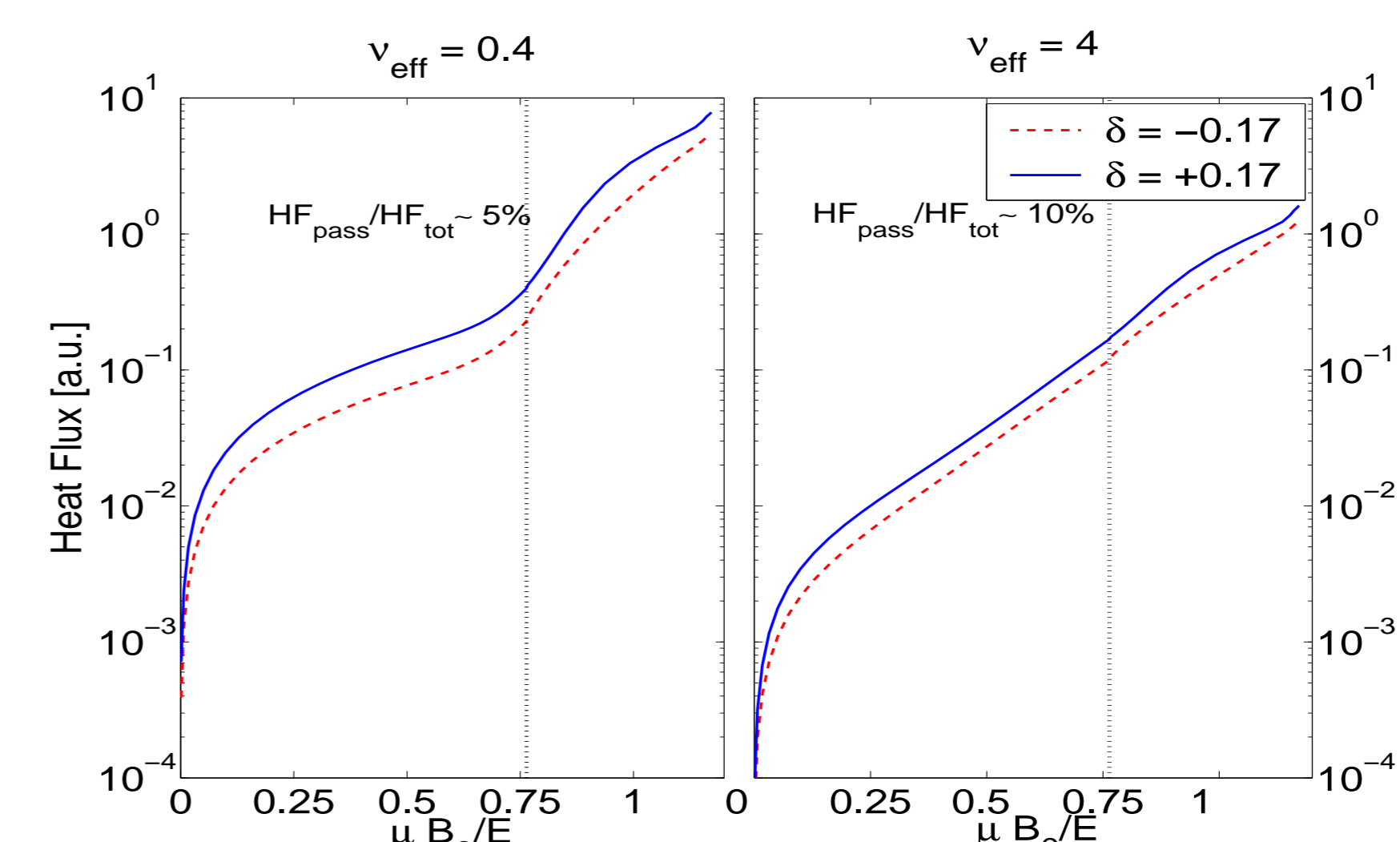
Solid curve: ratio of experimental electron thermal conductivities, as a function of the square root of the normalized volume, between discharges with edge triangularities equal to 0.4 and -0.4. •: same ratio simulated by GS2: the mean values and their uncertainties are calculated in the saturated phase of the simulation.

Investigation of instability drives

- Linearly most unstable modes propagate in the electron diamagnetic direction
- Linearly most unstable modes peak in the region $k_{\perp} \rho_i < 1$
- Non-linear heat flux is dominated by the electron species contribution
- The heat flux is dominated by trapped electrons over passing electrons

TCV shots under investigation are dominated by Trapped Electron Mode (TEM) turbulence

- Collisionality dependence is explained by collisional de-trapping mechanisms



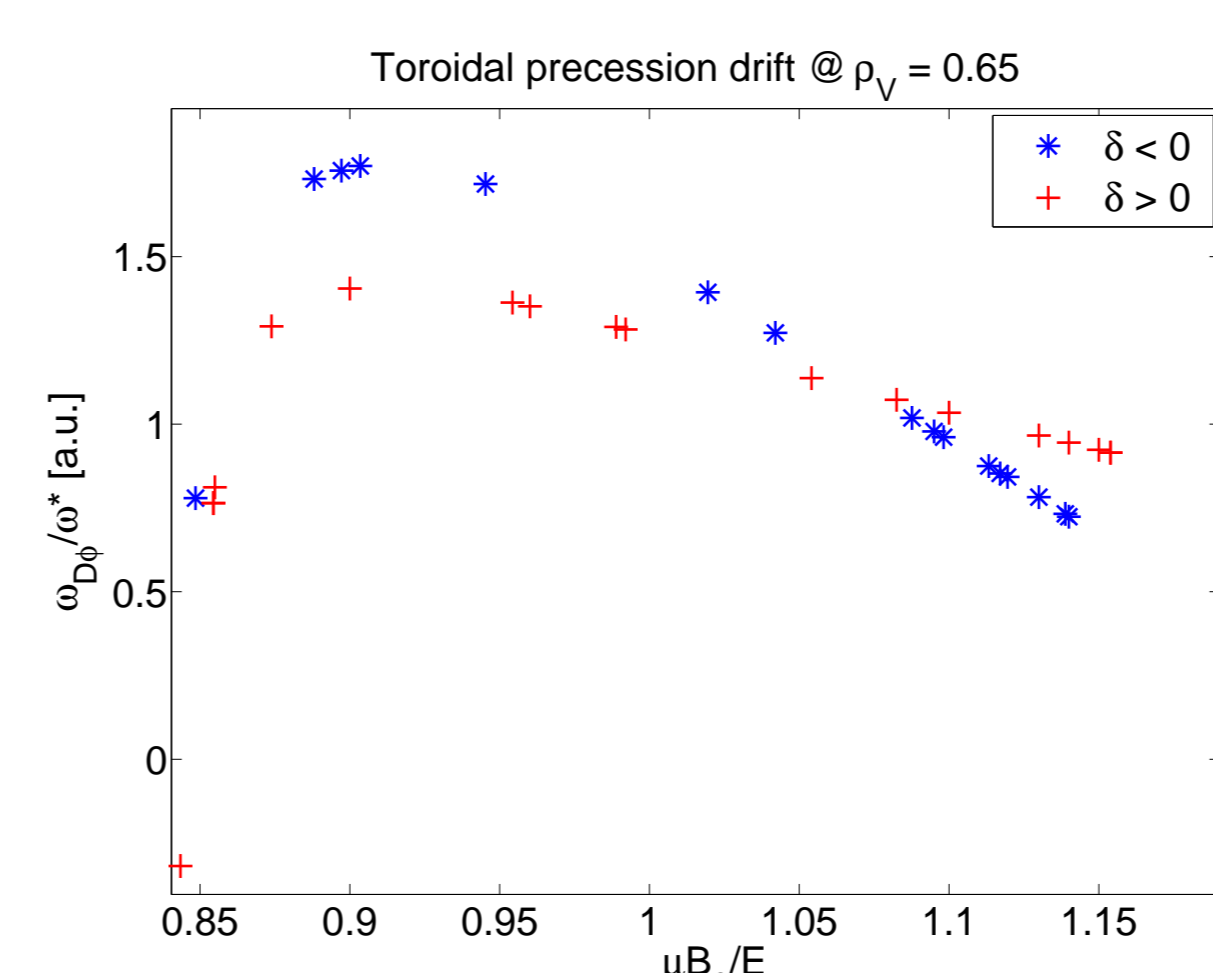
Heat Flux integrated over pitch angle against pitch angle for two values of collisionality. At higher ν_{eff} the relative passing contribution to the total flux increases. Note how negative δ stabilizes also passing electrons, even though their contribution to the total flux is negligible. The dotted vertical lines indicate the passing-trapped boundary.

- TEM are driven by the toroidal precession drift
- Magnetic drifts make the difference other parameters being equal (e.g. scale lengths)
- Linear simulations performed replacing specific drives in the GK equations indicate the curvature and ∇B drifts, together with the gradient of the ballooning eikonal, as responsible for discrepancy between positive and negative triangularity cases

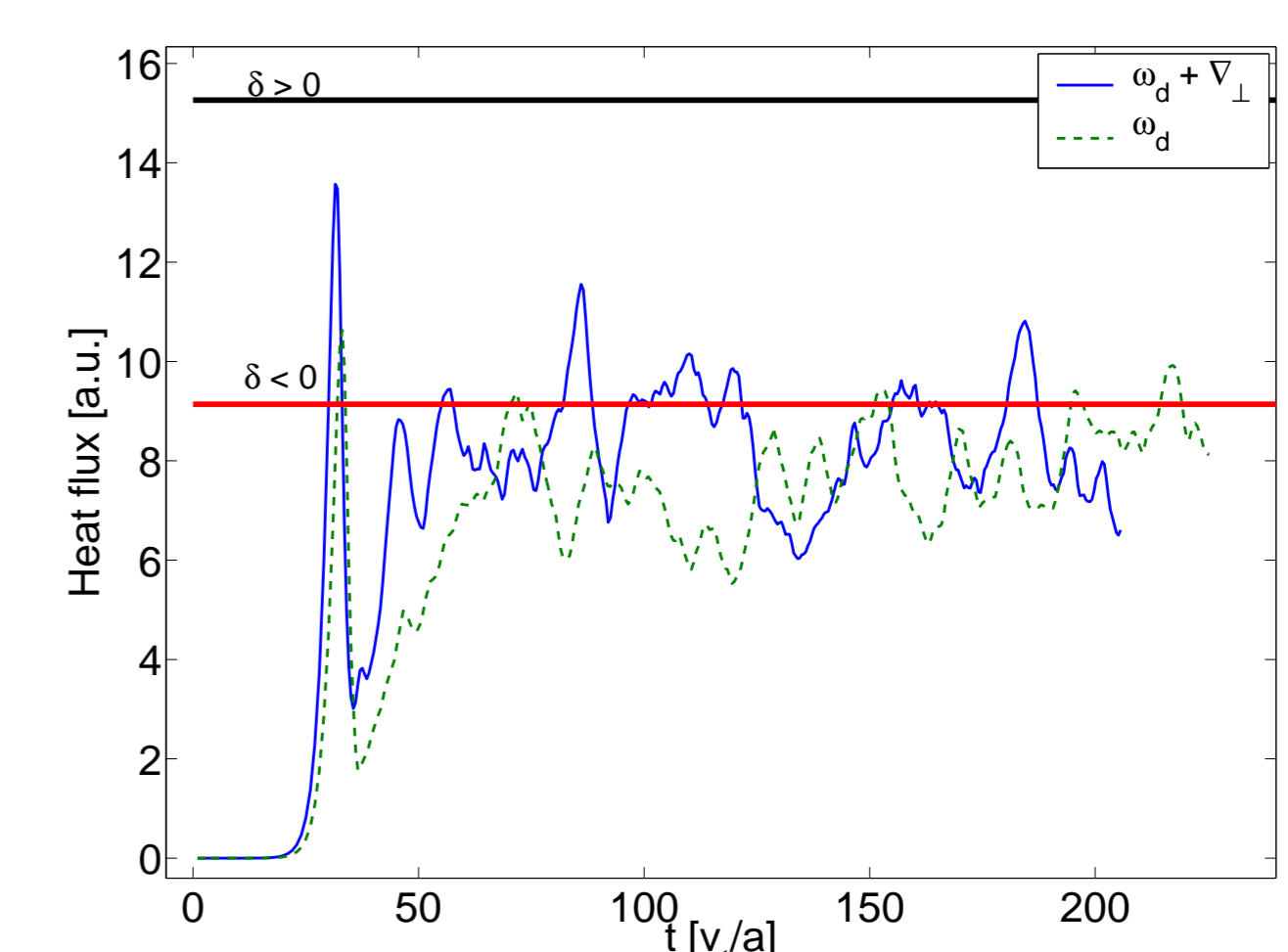
$$\frac{\delta = 0.17}{1} \quad \frac{\delta = -0.17}{0.77} \quad \frac{\omega_d}{0.90} \quad \frac{\omega_d + \nabla_{\perp}}{0.74} \quad \frac{\omega_d + \nabla_{\parallel}}{0.92} \quad \frac{\nabla_{\perp}}{0.82} \quad \frac{\nabla_{\perp} + \nabla_{\parallel}}{0.84} \quad \frac{\nabla_{\parallel}}{0.98}$$

Mixing length diffusivity estimate, normalized to the positive triangularity case, for a number of linear GS2 simulations performed after replacing individual drive terms of the positive triangularity equilibrium with the corresponding terms of the negative triangularity case.

- Initial non-linear simulations seem to confirm this hypothesis



Toroidal precession drift calculated by the Venus code[4] for two different triangularities. Deeply trapped particles are stabilized by a negative δ configuration, while the opposite happens for barely trapped particles.



Electron heat flux calculated for a positive δ equilibrium with individual terms replaced by the corresponding terms in the negative δ case. The black line represents the mean value of the actual positive δ case while the red line stands for the negative δ one.

Conclusions

- Negative triangularity tends to stabilize TEM through perpendicular drifts and flux surface topology
- Collisionality stabilizes TEM through de-trapping irrespective of triangularity
- Non-linear terms tend to be important in calculating actual diffusivity values

Acknowledgments

The authors would like to thank Dr. Paolo Ricci for useful discussions, Dr. Trach-Minh Tran and Dr. Alberto Bottino for valuable assistance and the authors of the GS2 code for releasing the source. Simulations were performed on the Linux clusters PLEIADES and PLEIADES2 of the Ecole Polytechnique Fédérale de Lausanne. This work was supported in part by the Swiss National Science Foundation.

References

- [1] Y. Camenen, A. Pochelon et al., Nucl. Fusion **47** (2007) 510
- [2] M. Kotschenreuther et al., Comput. Phys. Commun. **88** (1995) 128
- [3] F. Jenko et al., Plasma Phys. Contr. Fusion **47** (2005) B195
- [4] O. Fischer et al., Nucl. Fusion **42** (2002) 817